

# Controlling spin without magnetic fields: the Bloch-Rashba rotator

C.E. Creffield

*Departamento de Física de Materiales, Universidad Complutense de Madrid, E-28040 Madrid, Spain*

(Dated: September 3, 2020)

We consider the dynamics of a quantum particle held in a lattice potential, and subjected to a time-dependent spin-orbit coupling. Tilting the lattice causes the particle to perform Bloch oscillations, and by suitably changing the Rashba interaction during its motion, the spin of the particle can be gradually rotated. Even if the Rashba coupling can only be altered by a small amount, large spin-rotations can be obtained by accumulating the rotation from successive oscillations. We show how the time-dependence of the spin-orbit coupling can be chosen to maximize the rotation per cycle, and thus how this method can be used to produce a precise and controllable spin-rotator, which we term the Bloch-Rashba rotator, without requiring an applied magnetic field.

## I. INTRODUCTION

Spintronics<sup>1</sup> is a rapidly developing field of study, in which information is carried by an electron's spin as well as its charge. Spin qubits not only have the benefit of long spin coherence times, but their lower energy scales also promise lower-power, higher-speed devices. Their implementation, however, requires a method of manipulating the spin of individual electrons. This can be done by using micromagnets<sup>2–6</sup>, but it is difficult to confine magnetic fields to the small volumes occupied by the qubits and obtain the necessary level of control. A method of addressing spin by applying local gating potentials would thus be greatly preferable. A possible means to achieve this is provided by spin-orbit coupling (SOC). This is a relativistic effect in which an electric field is transformed into an effective magnetic field in the rest-frame of the electron, which then interacts with the electron's spin, coupling it to the particle's momentum. In condensed matter systems, SOC underlies the existence of topological insulators<sup>7</sup>, and provides the basis of the spin quantum Hall effect<sup>8</sup>.

If the electric field arises from inversion asymmetry in the crystal lattice itself, the SOC is termed Dresselhaus coupling. Alternatively, if it arises from spatial inhomogeneity of a heterostructure interface, it is called Rashba coupling<sup>9,10</sup>. The Rashba effect is particularly suitable for qubit manipulation because the magnitude of the coupling can be tuned by electrostatic gates<sup>11,12</sup>. An electron's spin can thus be rotated by moving an electron in space while controlling the size of the Rashba coupling<sup>13</sup>. In a quantum wire, for example, a spin-flip can be obtained<sup>14</sup> by allowing an electron to move a certain distance along the wire, where the required distance<sup>15</sup> is inversely related to the strength of the coupling.

It would, however, be more convenient to be able to transport the electron back to its original location, so that having been rotated by a certain angle it can then be used for further quantum logic operations. This requires time-dependent control of the Rashba coupling<sup>16–21</sup>, otherwise the rotation-angle obtained on the outward leg of the electron's journey would be unwound by the re-

turn leg. In Ref.<sup>22</sup> a method to achieve this was proposed, where an electron trapped in a local potential was moved along a closed trajectory in space, while the Rashba coupling was varied in time, to obtain the desired spin-rotation. An appealing aspect of this system is that exact analytical solutions can be obtained<sup>23–25</sup>, allowing its robustness towards gate noise<sup>26</sup> and thermal effects<sup>27</sup> to be assessed.

In this paper we consider inducing a spin-rotation in a conceptually similar way, but instead we use a lattice system. This could be produced by applying a superlattice potential to a quantum wire, or by suitably gating a heterostructure. A lattice system provides several advantages. Unlike the continuum case, a localized wavepacket can be put into oscillatory motion by tilting the lattice<sup>28,29</sup> to generate Bloch oscillations<sup>30,31</sup>, avoiding the need to carry the electron from place to place in a trap. Furthermore, the wavepacket will not be excited out of its ground state by the motion<sup>22</sup>, avoiding a possible source of noise. By adjusting the Rashba coupling in phase with the Bloch oscillations, we will show how it is possible to controllably rotate the spin of an electron, thereby forming a “Bloch-Rashba rotator”. Even if the Rashba coupling can only be varied by a small amount, a large spin-rotation can be built up by allowing the particle to undergo several oscillations, allowing the rotation angle to accumulate little by little.

## II. BLOCH-RASHBA HAMILTONIAN

We consider a one-dimensional wire lying on a two-dimensional interface in the  $x - y$  plane, subject to a Rashba SOC governed by an electric field perpendicular to the interface. For convenience we will take the wire to be aligned along the  $x$ -direction. In a continuum, the Rashba Hamiltonian will be given by  $H_R = \alpha(E_z)/\hbar (\boldsymbol{\sigma} \times \mathbf{p})_z$ <sup>10</sup>, where  $\alpha$  is the Rashba coupling, regulated by the applied electric field  $E_z$ ,  $\sigma_j$  are the Pauli spin-operators, and  $\mathbf{p}$  is the particle's momentum. Moving to a lattice description, the continuum Hamiltonian,

$H = p^2/2m^* + H_R$ , becomes a tight-binding model<sup>32</sup>

$$H_{\text{latt}} = - \sum_j J \left[ c_j^\dagger c_{j+1} + \text{H.c.} \right] + J_{\text{so}} \left[ c_j^\dagger (i\sigma_y) c_{j+1} + \text{H.c.} \right] \quad (1)$$

where  $c_j^\dagger = (c_{j\uparrow}^\dagger, c_{j\downarrow}^\dagger)$ , and  $c_{j\sigma}^\dagger / c_{j\sigma}$  is the creation / annihilation operator for a fermion of spin  $\sigma$  on lattice site  $j$ . In this expression,  $J$  represents the single-particle tunneling between adjacent lattice sites, and  $J_{\text{so}}$  is the spin-orbit tunneling produced by the Rashba SOC, whose amplitude is proportional to  $\alpha$ . Clearly the SOC term will induce a rotation of the electron spin around the  $S_y$  axis when the particle moves along the lattice, that is, the spin-rotation will be about an axis perpendicular to both the direction of motion and the direction of the electric field.

A convenient way to represent the hopping terms in Eq. 1 is to visualize them in terms of the Creutz ladder<sup>33</sup>, as shown in Fig. 1a. In this picture, spin-up fermions occupy sites on the top edge of the ladder, while sites on the lower edge hold spin-down fermions. The single-particle tunneling terms do not change the spin of a fermion, and so they represent hopping processes along the edges of the ladder, shown by the black lines. The tunneling terms governed by  $J_{\text{so}}$ , however, involve a spin-flip, and so are represented by the diagonal red lines connecting sites on the two edges of the ladder.

The dispersion relation of Hamiltonian (1) is shown in Fig. 1b. When the Rashba coupling vanishes ( $J_{\text{so}} = 0$ ) we recover the standard cosinusoidal dispersion relation for a single-band tight-binding model, each state having a two-fold spin degeneracy. As  $J_{\text{so}}$  increases, the degeneracy between spin-up and spin-down states is lifted, and the spectrum splits into two bands, each displaced from the origin by a momentum proportional to the Rashba coupling  $J_{\text{so}}$ .

Having obtained the lattice Hamiltonian (1), the next step is to introduce a tilt to the lattice potential, as shown in Fig. 2. This is described by the Bloch-Rashba Hamiltonian

$$H_{\text{BR}} = H_{\text{latt}} + V_0 \sum_j j n_j, \quad (2)$$

where  $V_0$  is the difference in potential between neighboring sites, and  $n_j$  is the standard number operator. Classically one would expect a particle held in in a tilted potential to roll down the slope and thus accelerate uniformly to the right. Quantum effects produced by the lattice, however, complicate this simple picture, and the wavepacket instead undergoes a coherent oscillation<sup>34</sup> termed Bloch oscillation, whose frequency and amplitude depend on the lattice tilt. If the initial wavepacket is well-localized in space, the position of its center of mass<sup>34,35</sup> is given by the simple expression

$$x(t) = 2(J/V_0) (1 - \cos V_0 t). \quad (3)$$

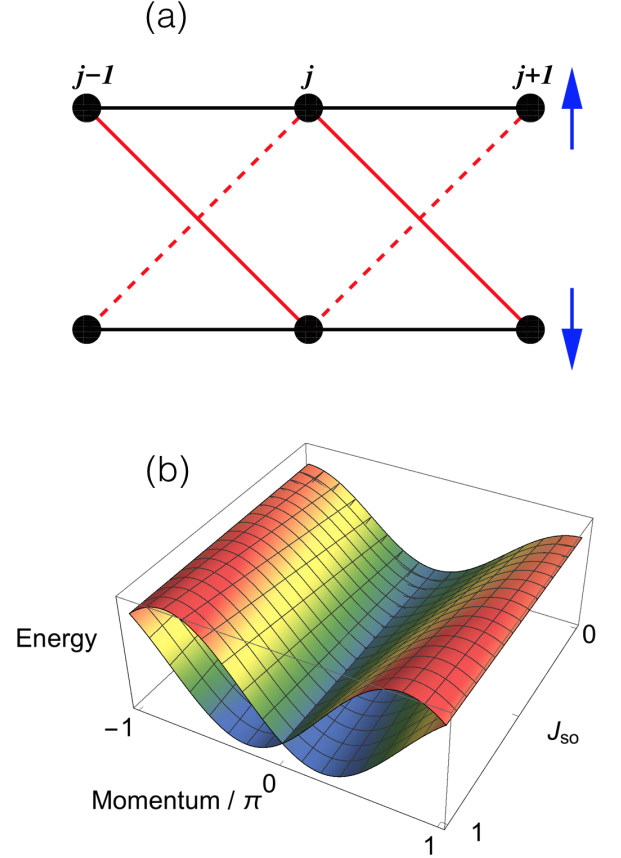


FIG. 1. (a) Creutz ladder representation of the lattice Hamiltonian (1). The index  $j$  labels the sites of the lattice. Black lines along the edges of the ladder represent standard single-particle hopping between neighboring sites which conserves the spin-orientation. Diagonal hopping terms (shown in red) represent processes in which a particle hops by one lattice site and flips its spin, which arise from the Rashba interaction. The red dotted / solid lines have amplitudes of  $-J_{\text{so}} / J_{\text{so}}$ , due to the  $\sigma_y$  term in  $H_{\text{latt}}$ . (b) Dispersion relation of the lattice Hamiltonian. For  $J_{\text{so}} = 0$  the system exhibits the standard single-band dispersion relation  $E_k = -2J \cos k$ . As  $J_{\text{so}}$  is increased, the spectrum splits into two cosinusoidal bands, displaced from the origin by an amount proportional to the spin-orbit coupling.

### III. RESULTS

#### A. Constant SOC

In Fig. 3 we show the time evolution of a Gaussian wavepacket placed in a lattice with a small tilt of  $V_0 = 0.01J$ . The width of the Gaussian,  $\sigma^2 = 1000a^2$ , where  $a$  is the lattice spacing, was chosen to be sufficiently small for the wavepacket to be well-localized in space, but large enough for it to exhibit well-defined Bloch oscillations; note that a very narrow wavepacket would instead experience Wannier-Stark localization<sup>34</sup>.

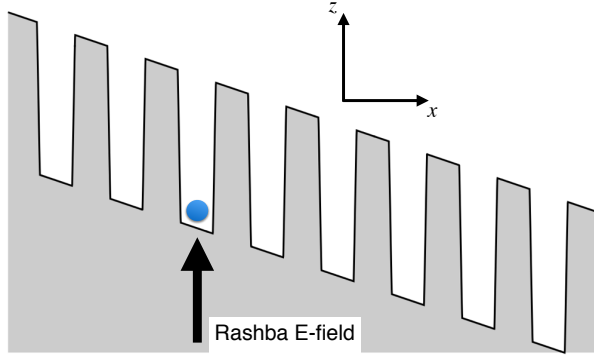


FIG. 2. Schematic form of the Bloch-Rashba rotator. A particle is placed in a lattice which is subjected to a small tilt causing the particle to undergo an oscillatory motion through the lattice (Bloch oscillation). An external electric field regulates the Rashba spin-orbit coupling, causing the spin of the particle to rotate about an axis mutually perpendicular to its motion and the Rashba field. We consider the particle motion to be in the  $x$ -direction, while the Rashba field is aligned with the  $z$ -axis; consequently the particle spin will rotate about the  $y$ -axis, in the  $S_x - S_z$  plane.

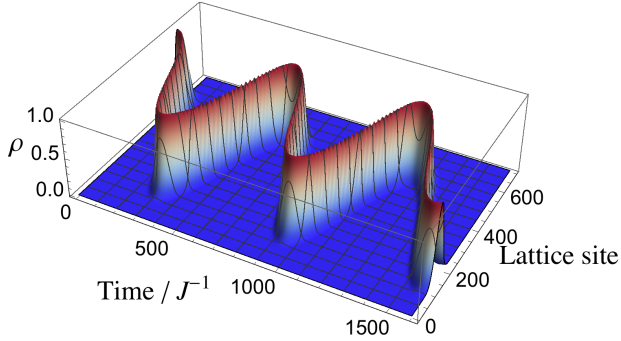


FIG. 3. A Gaussian wavepacket placed in a tilted lattice potential makes an oscillatory motion along the lattice. The amplitude of the oscillation and its frequency are governed by the size of the tilt, Eq. 3. The lattice tilt used here,  $V_0 = 0.01J$ , gives a Bloch period of  $T_B = 200\pi/J$ .

The system was numerically integrated in time under the lattice Hamiltonian (2), and the plot displays the particle density,  $\rho(x, t) = |\psi(x, t)|^2$ . It can be seen that the wavepacket oscillates along the lattice as expected, while retaining its Gaussian shape, clearly displaying Bloch oscillations.

In Fig. 4a we show this motion more quantitatively, by plotting the motion of the center of mass of the system. From Eq. 1, we can see that the motion of the particle will be associated with a rotation of its spin about the  $S_y$ -axis. Thus if the particle is initialized in a spin-up

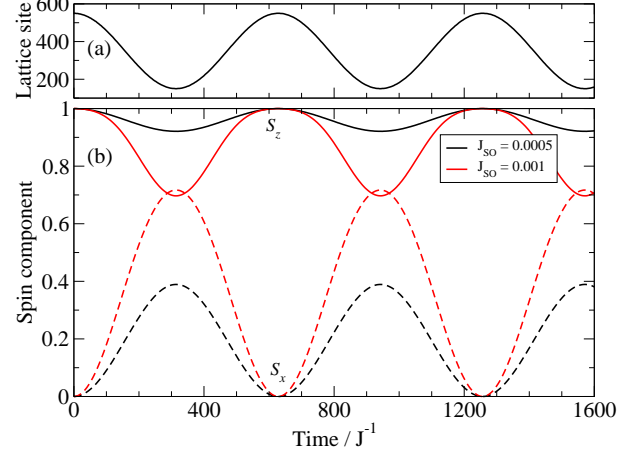


FIG. 4. (a) Bloch oscillation of the Gaussian wavepacket. The center of mass of the wavepacket makes a sinusoidal oscillation along the lattice, the period of which is determined by the lattice tilt,  $T_B = 2\pi/V_0$  (see Eq. 3). b) Solid lines denote  $\langle S_z \rangle$ , the dashed lines denote  $\langle S_x \rangle$ . The  $x$  and  $z$  components of the particle's spin oscillate sinusoidally in time, with the same period as the Bloch oscillation. When the SOC is increased from  $J_{so} = 0.0005J$  (black lines) to  $J_{so} = 0.001$  (red lines), the amplitude of the oscillations in  $\langle S_x \rangle$  and  $\langle S_z \rangle$  correspondingly increases.

state, during its motion through the lattice, its spin will rotate in the  $S_x - S_z$  plane. In Fig. 4b we plot the expectation values of the spin projections  $\langle S_z \rangle$  and  $\langle S_x \rangle$  for two different values of the Rashba SOC. We can see that in each case,  $\langle S_z \rangle$  takes an initial value of one, as expected, and then decreases as the particle moves through the lattice. At the same time  $\langle S_x \rangle$  increases from zero. After reaching the extremum of its motion, the particle reverses its direction and returns to its initial position. In this portion of its motion the values of  $\langle S_z \rangle$  and  $\langle S_x \rangle$  return smoothly to their initial values. The spin of the particle thus rotates periodically in the  $S_x - S_z$  plane, with the same period as the Bloch oscillation. In the inset of Fig. 5 we plot the evolution of the particle's spin in this plane. We can note that the modulus of the spin remains approximately constant, indicating that the spin vector is evolving smoothly along a circle on the surface of the Bloch sphere, as required. Close examination of this trajectory, however, reveals minor deviations from the circle, corresponding to a periodic “breathing” motion of the wavepacket's width during the Bloch oscillation. As mentioned previously, the rotation angle acquired in the first part of the oscillation is exactly canceled when the particle returns to its original position, and so the Bloch vector only traces out a small, retracing arc on the Bloch sphere. To obtain a net rotation it is necessary to also vary the SOC with time, and so consider a *two-parameter* driving.

## B. Time-dependent SOC

The simplest form of varying the SOC to produce a net spin-rotation is for it to take two different values<sup>24</sup>: one during the outward motion of the Bloch oscillation, and another value while the particle returns. In Fig. 5 we show the time-dependence of  $\langle S_z \rangle$  for this driving protocol, where  $J_{\text{so}}$  is set to zero on the return leg. Initially the behaviour of  $\langle S_z \rangle$  follows that of the system considered previously, but on the return leg the value of  $\langle S_z \rangle$  is quenched. If  $J_{\text{so}}$  is then periodically restored and quenched in this way, in phase with the Bloch oscillation, the time-evolution of  $\langle S_z \rangle$  will show a staircase behavior. Thus even if  $J_{\text{so}}$  is limited to a small maximum value, a large spin-rotation can nonetheless be obtained by allowing the particle to accumulate the rotation angle over many Bloch oscillations, as can also be seen in the inset of the figure.

Clearly the spin-rotation will occur more rapidly if the spin is able to continue rotating in the same sense on the return leg of the cycle, rather than just being frozen. As the Rashba SOC has the schematic form  $H_R = \alpha \sigma_y p$ , we can see that this can be done by reversing the sign of the coupling,  $\alpha \rightarrow -\alpha$ , to compensate for the reversal of the particle's momentum. The time evolution produced by this “flipped” protocol (where the sign of  $J_{\text{so}}$  is flipped in each half-period of the Bloch oscillation) is also shown in Fig. 5, and indeed demonstrates how the rotation occurs more quickly, the spin-rotation accumulating twice as quickly as in the quenched protocol.

As well as using discrete values of  $J_{\text{so}}$ , it is also possible to vary the SOC continuously in time. In Fig. 5 we show the result of sinusoidally modulating  $J_{\text{so}}$  with the same period as the Bloch oscillation,  $J_{\text{so}} = J_0 \sin(\omega_B t)$ . In this case, as in the case of the “flipped driving”, the spin-rotation continues in the same sense in both halves of the Bloch oscillation. As a result the rotation angle increases at a comparable, though slower, rate to that of the case of flipped driving.

To compare the efficacy of the different driving protocols, it is informative to look at the trajectory traced out in the displacement- $J_{\text{so}}$  parameter space. The net spin-rotation achieved after one cycle of driving (one Bloch oscillation) is proportional to the area enclosed by this trajectory<sup>23,26</sup>. We show the four cases that we have considered in Fig. 6. When  $J_{\text{so}}$  is held constant, the trajectory just traces a straight line (Fig. 6a) which encloses no area, and thus corresponds to no net spin-rotation. In the quenching protocol (Fig. 6b),  $J_{\text{so}}$  takes two values and the trajectory traces out a rectangle. If  $J_{\text{so}}$  is restricted to take only positive values, this form of driving clearly maximizes the possible area enclosed, and so will be the most effective. If  $J_{\text{so}}$  can take both positive and negative values then the flipped driving will be the most effective, enclosing double the area of the quenched driving protocol. Finally, the sinusoidal driving traces out a circular trajectory in this parameter-space. Although the rotation per cycle is less than for flipped driving, it

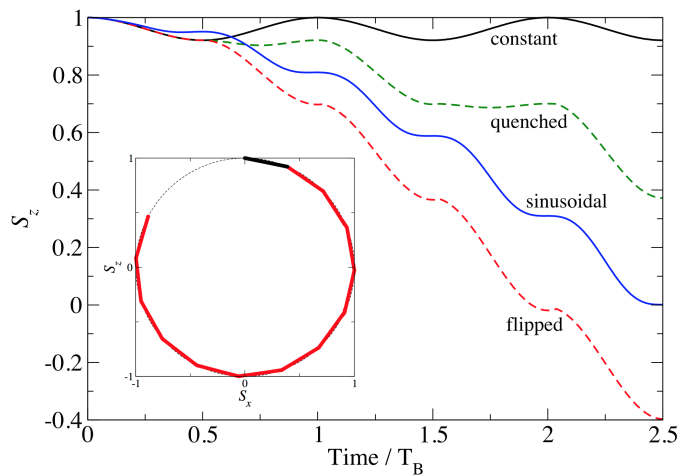


FIG. 5. The spin projections,  $\langle S_x \rangle$  and  $\langle S_z \rangle$  as a function of time. When the Rashba tunneling,  $J_{\text{so}}$ , is held constant, the electron spin rotates at a constant rate while the electron wavepacket propagates in one direction through the lattice. However, when the wavepacket reverses to complete a cycle of Bloch oscillation, the spin retraces its trajectory to its original configuration, and so no spin-rotation is acquired. When  $J_{\text{so}}$  is quenched to zero during the second half of the Bloch cycle, the electron spin is frozen, and so does not retrace its trajectory. Accordingly the rotation angle changes in steps as the Bloch oscillation continues. Flipping the sign of the Rashba tunneling,  $J_{\text{so}} \rightarrow -J_{\text{so}}$  in the second half-cycle causes the spin to continue rotating at the same rate during the entire Bloch oscillation.  $J_{\text{so}}$  can also be varied continuously,  $J_{\text{so}} = J_0 \sin \omega_B t$ , with the same frequency as the Bloch oscillation, to achieve this effect. Inset: When  $J_{\text{so}}$  is held constant, the Bloch vector oscillates over a small range (black symbols). By making  $J_{\text{so}}$  time-dependent, the Bloch vector can now progressively step around a great circle in the  $S_x - S_z$  plane.

is of similar order.

## IV. CONCLUSIONS

We have shown how the interplay between Bloch oscillations and the SOC can be used to create a controllable spin rotator, that does not require an externally applied magnetic field. In contrast to previous proposals, the electron does not have to be transported in a moving potential well, but its motion is instead an intrinsic property of the lattice system. We have shown how the system can be conveniently mapped to the Creutz ladder, and how the spin-rotation produced per cycle can be optimized by maximizing the area enclosed by the trajectory in the  $x - J_{\text{so}}$  parameter space.

In a doped InAs heterostructure, it was found that the Rashba SOC could be enhanced by a factor of 1.5<sup>11</sup> by applying a gate voltage of a few volts, while enhancement of up to a factor of six could be obtained in an InAs

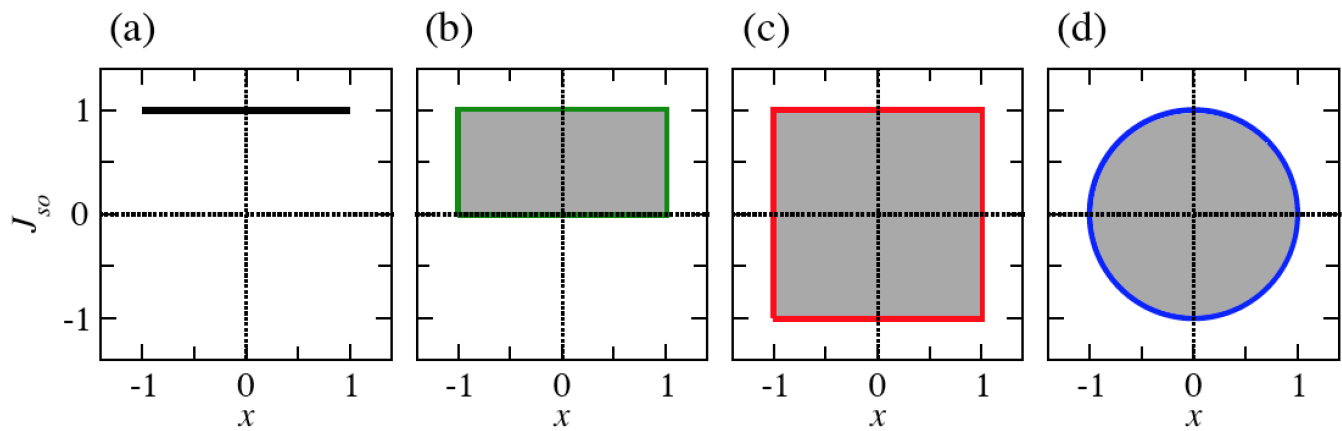


FIG. 6. Area enclosed in the parameter plane ( $x - J_{so}$ ) for the different protocols shown in Fig. 5. The displacement  $x$  is measured in units of the amplitude of the Bloch oscillation. (a) Constant  $J_{so}$ . The trajectory is a straight line; as it does not enclose an area, the net spin-rotation is zero. (b) Quenched driving.  $J_{so}$  takes two values,  $J_{so} = 1$  in the first half-period, and  $J_{so} = 0$  in the second, so the trajectory encloses a rectangle. (c) Flipped driving.  $J_{so}$  again takes two values, but is now negative ( $J_{so} = -1$ ) in the second half-period. The area again is again rectangular, but encloses twice the area obtained for quenched driving. As a consequence the spin rotates more rapidly. (d) Sinusoidal driving. The trajectory now encloses a circle.

quantum wire<sup>12</sup>. Ferroelectric Rashba materials<sup>36–38</sup> also hold out the prospect of having large, electrically controllable Rashba couplings. However, even if the Rashba coupling of a material can only be changed by a small amount, the method described here allows large values of spin-rotation to be achieved by letting a particle undergo several periods of Bloch oscillation, and allowing the rotation to accumulate. As well as applying to solid state materials, an exciting possibility is to use this technique to manipulate ultracold quantum gases. In such systems an effective Rashba coupling can be engineered by dressing atomic spin states with lasers<sup>39</sup>, and a lattice structure can be imposed by applying an optical lattice potential<sup>40,41</sup>. These systems are extremely clean and controllable, and would provide an ideal format to investigate this form of spin control.

In this work we have just considered a one-dimensional

system, and consequently the spin-rotation only occurs in the  $S_x - S_z$  plane. To obtain full coverage of the Bloch sphere, it would be necessary for the particle to move in a perpendicular direction as well. This could be achieved by applying a two-dimensional lattice potential, in which Bloch oscillations could be induced in the two directions. Extending the model to treat this situation, and including the effects of noise and dissipation, are fascinating subjects for future study.

## ACKNOWLEDGMENTS

This work has been supported by Spain's MINECO through grant FIS2017-84368-P. The author thanks Toni Ramšak for introducing him to this to this problem, and Gloria Platero for stimulating discussions.

- <sup>1</sup> I. Žutić, J. Fabian, and S. Das Sarma, *Rev. Mod. Phys.* **76**, 323 (2004).
- <sup>2</sup> Y. Tokura, W. G. van der Wiel, T. Obata, and S. Tarucha, *Phys. Rev. Lett.* **96**, 047202 (2006).
- <sup>3</sup> F. H. L. Koppens, C. Buizert, K. J. Tielrooij, I. T. Vink, K. C. Nowack, T. Meunier, L. P. Kouwenhoven, and L. M. K. Vandersypen, *Nature* **442**, 766 (2006).
- <sup>4</sup> M. Pioro-Ladrière, T. Obata, Y. Tokura, Y. S. Shin, T. Kubo, K. Yoshida, T. Taniyama, and S. Tarucha, *Nature Physics* **4**, 776 (2008).
- <sup>5</sup> F. Forster, M. Mühlbacher, D. Schuh, W. Wegscheider, and S. Ludwig, *Phys. Rev. B* **91**, 195417 (2015).
- <sup>6</sup> A. Bayat, C. E. Creffield, J. H. Jefferson, M. Pepper, and S. Bose, *Semiconductor Science and Technology* **30**, 105025 (2015).

- <sup>7</sup> M. Z. Hasan and C. L. Kane, *Rev. Mod. Phys.* **82**, 3045 (2010).
- <sup>8</sup> M. König, S. Wiedmann, C. Brüne, A. Roth, H. Buhmann, L. W. Molenkamp, X.-L. Qi, and S.-C. Zhang, *Science* **318**, 766 (2007).
- <sup>9</sup> E. I. Rashba, *Sov. Phys. Solid. State* **2**, 1109 (1960).
- <sup>10</sup> Y. A. Bychkov and E. I. Rashba, *Journal of Physics C: Solid State Physics* **17**, 6039 (1984).
- <sup>11</sup> J. Nitta, T. Akazaki, H. Takayanagi, and T. Enoki, *Phys. Rev. Lett.* **78**, 1335 (1997).
- <sup>12</sup> D. Liang and X. P. A. Gao, *Nano Letters* **12**, 3263 (2012).
- <sup>13</sup> E. I. Rashba and A. L. Efros, *Phys. Rev. Lett.* **91**, 126405 (2003).
- <sup>14</sup> C. Flindt, A. S. Sørensen, and K. Flensberg, *Phys. Rev. Lett.* **97**, 240501 (2006).

- <sup>15</sup> W. Häusler, *Journal of Superconductivity* **16**, 309 (2003).
- <sup>16</sup> F. Liang, Y. H. Yang, and J. Wang, *The European Physical Journal B* **69**, 337 (2009).
- <sup>17</sup> Y. Avishai, D. Cohen, and N. Nagaosa, *Phys. Rev. Lett.* **104**, 196601 (2010).
- <sup>18</sup> A. López, Z. Z. Sun, and J. Schliemann, *Phys. Rev. B* **85**, 205428 (2012).
- <sup>19</sup> H. Pan and Y. Zhao, *Journal of Applied Physics* **111**, 083703 (2012).
- <sup>20</sup> A. López, A. Scholz, Z. Z. Sun, and J. Schliemann, *The European Physical Journal B* **86**, 366 (2013).
- <sup>21</sup> J. Pawłowski, P. Szumniak, and S. Bednarek, *Phys. Rev. B* **93**, 045309 (2016).
- <sup>22</sup> T. Čadež, J. H. Jefferson, and A. Ramšak, *New Journal of Physics* **15**, 013029 (2013).
- <sup>23</sup> T. Čadež, J. H. Jefferson, and A. Ramšak, *Phys. Rev. Lett.* **112**, 150402 (2014).
- <sup>24</sup> A. Kregar, J. H. Jefferson, and A. Ramšak, *Phys. Rev. B* **93**, 075432 (2016).
- <sup>25</sup> A. Ramšak, T. Čadež, A. Kregar, and L. Ulčakar, *The European Physical Journal Special Topics* **227**, 353 (2018).
- <sup>26</sup> L. Ulčakar and A. Ramšak, *New Journal of Physics* **19**, 093015 (2017).
- <sup>27</sup> B. Donvil, L. Ulčakar, T. c. v. Rejec, and A. Ramšak, *Phys. Rev. B* **101**, 205427 (2020).
- <sup>28</sup> F. Bloch, *Zeitschrift für Physik* **52**, 555 (1929).
- <sup>29</sup> C. Zener, *Proceedings of the Royal Society of London A: Mathematical, Physical and Engineering Sciences* **145**, 523 (1934).
- <sup>30</sup> J. Feldmann, K. Leo, J. Shah, D. A. B. Miller, J. E. Cunningham, T. Meier, G. von Plessen, A. Schulze, P. Thomas, and S. Schmitt-Rink, *Phys. Rev. B* **46**, 7252 (1992).
- <sup>31</sup> C. Waschke, H. G. Roskos, R. Schwedler, K. Leo, H. Kurz, and K. Köhler, *Phys. Rev. Lett.* **70**, 3319 (1993).
- <sup>32</sup> M. Dey, S. K. Maiti, and S. N. Karmakar, *Journal of Applied Physics* **109**, 024304 (2011).
- <sup>33</sup> M. Creutz, *Phys. Rev. Lett.* **83**, 2636 (1999).
- <sup>34</sup> T. Hartmann, F. Keck, H. J. Korsch, and S. Mossmann, *New Journal of Physics* **6**, 2 (2004).
- <sup>35</sup> M. Holthaus, *Journal of Optics B: Quantum and Semiclassical Optics* **2**, 589 (2000).
- <sup>36</sup> A. Narayan, *Phys. Rev. B* **92**, 220101 (2015).
- <sup>37</sup> J. Varignon, J. Santamaria, and M. Bibes, *Phys. Rev. Lett.* **122**, 116401 (2019).
- <sup>38</sup> C. Autieri, P. Barone, J. Ślawińska, and S. Picozzi, *Phys. Rev. Materials* **3**, 084416 (2019).
- <sup>39</sup> Y. J. Lin, K. Jiménez-García, and I. B. Spielman, *Nature* **471**, 83 (2011).
- <sup>40</sup> Y. V. Kartashov, V. V. Konotop, D. A. Zezyulin, and L. Torner, *Phys. Rev. Lett.* **117**, 215301 (2016).
- <sup>41</sup> J. Larson, J.-P. Martikainen, A. Collin, and E. Sjöqvist, *Phys. Rev. A* **82**, 043620 (2010).